DOI: 10.1021/ma9007829

Macromolecules
ARTICLE

Evidence of Compartmentalization in Catalytic Chain Transfer Mediated Emulsion Polymerization of Methyl Methacrylate

Niels M. B. Smeets,[†,‡] Johan P. A. Heuts,[†] Jan Meuldijk,*[,†] Michael F. Cunningham,[‡] and Alex M. van Herk[†]

[†]*Department of Chemical Engineering and Chemistry, Eindhoven University of Technology, P.O. Box 513, 5600 MB Eindhoven, The Netherlands, and* [‡]*Department of Chemical Engineering, Queen's University, Dupuis Hall, 19 Division St., Kingston, Ontario, Canada K7L 3N6*

Received April 10, 2009; Revised Manuscript Received July 29, 2009

ABSTRACT: Evidence of compartmentalization of the catalytic chain transfer agent in seeded emulsion polymerization of methyl methacrylate (MMA) is shown experimentally. The addition of bis[(difluoroboryl)dimethylglyoximato]cobalt(II) (COBF) to seed particles swollen below their maximum saturation concentration exhibited multimodal molecular weight distributions (MWD) which are attributed to a statistical distribution of COBF molecules over the polymer particles. The experimental observations suggest that there are two limits for catalytic chain transfer in emulsion polymerization: (i) at the earlier stages of the polymerization where a global COBF concentration governs the MWD and (ii) at the latter stages of the polymerization where a statistical distribution of COBF molecules governs the MWD. To the best of our knowledge, these results are the first to suggest evidence of compartmentalization in catalytic chain transfer mediated emulsion polymerization.

Introduction

Compartmentalization in heterogeneous polymerization systems refers to two distinctive and opposite effects:[1,2] first, a segregation effect where radicals located in different particles are unable to react with each other and, second, a confined space effect where the reaction rate between two radicals in a particle increases with decreasing particle size. When compared to bulk polymerization, the high reaction rates and high average molecular weights in emulsion polymerization are due to the segregation of radicals. Strong compartmentalization behavior in emulsion polymerization can result in a scenario where there are only zero or one radical in a particle, when bimolecular termination is sufficiently fast. This scenario is also referred to as zero-one kinetics, in which the entry of a radical into a particle already containing one radical results in (pseudo)-instantaneous termination.[3,4] Both the rate of polymerization per particle and the average molecular weight of the polymer formed depend on the characteristic time of radical entry. In a second scenario, referred to as pseudobulk kinetics, the average number of radicals per particle ($\bar{n}$) is relatively large, and particles can contain more than one radical at a time. In this scenario the effects of compartmentalization are less pronounced.

Compartmentalization in emulsion polymerization is not restricted to radicals only. In recent years controlled/living radical polymerization has extended the range of polymer architectures obtainable from classic free radical polymerization.[5−8] Controlled/living radical polymerization techniques such as reversible addition−fragmentation chain transfer (RAFT), nitroxide-mediated polymerization (NMP), and atom transfer radical polymerization (ATRP) include the addition of an agent which controls the molecular weight of the polymer at the loci of polymerization, i.e., the polymer particles. Although compartmentalization in NMP[9−12] and ATRP[1,13] mediated emulsion polymerization refers to the compartmentalization of the controlling agent, and not to the segregation of radicals as in a conventional emulsion polymerization, it does affect the rate of polymerization and livingness of the system[9,13] (i.e., the average molecular weight obtained and the polydispersity index). Compartmentalization in catalytic chain transfer (CCT) mediated emulsion polymerization also affects the average molecular weight and polydispersity index; however, it differs from compartmentalization in controlled/living radical polymerization as it seems to be determined by mass transfer effects rather than by particle sizes.

CCT is a versatile method for robust molecular weight control.[14−20] In catalytic chain transfer mediated polymerizations, the radical activity is transferred from a propagating radical to a monomer molecule, yielding a dead polymer chain with a vinyl end-group functionality and a monomeric radical (Scheme 1). In the first step, the active Co(II) complex abstracts a hydrogen atom from the propagating polymer chain, resulting in a dead polymer chain and a Co(III)−H complex. Subsequently, the hydrogen atom is transferred from the Co(III)−H complex to a monomer molecule, regenerating the active Co(II) complex and yielding a monomeric radical capable of propagation.

Bulk and solution polymerizations are homogeneous reactions where the bis[(difluoroboryl)dimethylglyoximato]cobalt(II) (COBF) concentration in the locus of polymerization is equal to the overall COBF concentration in the reaction mixture. The number-average degree of polymerization (DP_n) can be predicted accurately by the Mayo equation[21] (eq 1), where $DP_{n,0}$ is the number-average degree of polymerization that would obtained in the absence of chain transfer agent, C_T is the chain transfer constant, and [M] is the monomer concentration.

$$\frac{1}{DP_n} = \frac{1}{DP_{n,0}} + C_T \frac{[COBF]}{[M]} \quad (1)$$

Because of the compartmentalized nature of the emulsion polymerization, the COBF concentration at the loci of the

*Corresponding author. E-mail: j.meuldijk@tue.nl.

 Published on Web 09/10/2009

Scheme 1. Overall Reaction of Catalytic Chain Transfer to Monomer

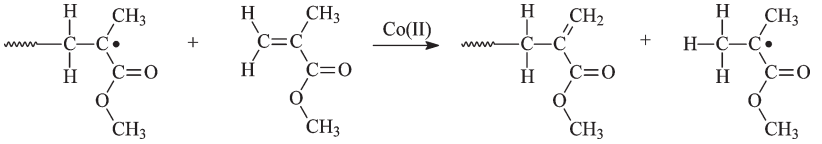

polymerization, i.e., the polymer particles, differs from the overall COBF concentration. Catalytic chain transfer mediated emulsion polymerizations with COBF often proceed in a regime where the ratio of number of COBF molecules and the number of polymer particles (N_{COBF}/N_p) < 1, depending on the partition coefficient (m_{Co}) and the phase ratio (β). In ab initio emulsion polymerization where the viscosity inside the polymer particles remains relatively low throughout the course of the polymerization, fast COBF mass transport between the polymer particles and the aqueous phase occurs. Monomodal molecular weight distributions are obtained with an instantaneous number-average degree of polymerization ($DP_{n,M}$) that can be predicted by the Mayo equation incorporating COBF partitioning[22] (eq 2).

$$DP_{n,m} = \frac{V_M[M]_p}{C_T}\frac{1}{N_{Co,0}}\left(\frac{m_{Co}\beta+1}{m_{Co}(\beta+1)}\right)\left(1+\frac{1}{\beta}\right) \qquad (2)$$

In this equation V_M is the total volume of the organic phase, $[M]_p$ the monomer concentration inside the polymer particles, $N_{Co,0}$ the absolute amount of COBF in moles, and C_T the intrinsic activity of COBF expressed as the chain transfer constant.

Fast exchange of COBF between the polymer particles results in a situation where a single COBF molecule is able to mediate multiple polymer particles, and hence there is an apparent COBF concentration over the entire organic phase. The Mayo equation, incorporating COBF partitioning, is valid in this situation and is able to successfully predict the instantaneous degree of polymerization.[22] However, if the mobility of the catalytic chain transfer agent is severely restricted, for instance in interval III of the polymerization when the viscosity of the polymer particles increases tremendously with conversion, compartmentalization of the catalytic chain transfer agent might occur, and this could affect the molecular weight distribution.

In the presented work we report evidence of compartmentalization effects in the catalytic chain transfer mediated emulsion polymerization of methyl methacrylate (MMA) with COBF. This catalytic chain transfer agent with considerable water solubility was used to exclude any transport limitations between the polymer particles and the aqueous phase.

Results and Discussion

Experimental Results. The number of COBF molecules per particle can be calculated if (i) the number of polymer particles is accurately known and (ii) if there are no monomer droplets present during the polymerization. Seeded emulsion polymerizations where the polymer particles are swollen below the saturation swelling concentration meet both requirements. The Vanzo equation can be used to estimate the amount of monomer required to swell the polymer particles to 85% of their saturation swelling.[23]

The partitioning behavior of COBF in a methyl methacrylate emulsion polymerization has been described before, and the instantaneous number-average degree of polymerization ($DP_{n,M}$) can be predicted accurately with the Mayo equation incorporating COBF partitioning (eq 2).[22,24] The partitioning behavior of COBF is expressed in terms of the partition coefficient $m_{Co} = [COBF]_M/[COBF]_W$ and the

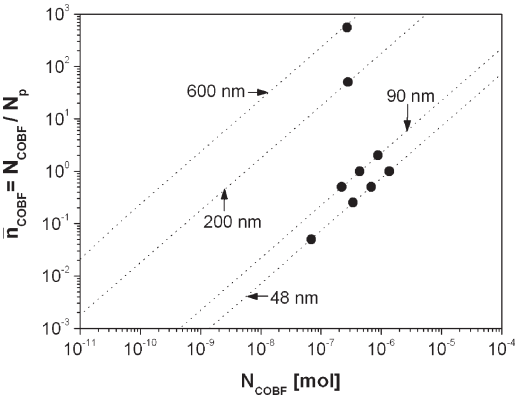

Figure 1. Average number of bis[(difluoroboryl)dimethylglyoximato (COBF) molecules per seed polymer particle for different particle diameters, i.e., 48, 90, 200, and 600 nm. Calculated $\bar{n}_{COBF}$ based on $m_{Co} = 0.72\ dm_W^3\ dm_M^{-3}$ and β based on eq 3 (···). Experiments as reported in this work (●).

Table 1. Latex Properties of the Methyl Methacrylate Emulsions Prepared by the Seeded Emulsion Polymerization of Methyl Methacrylate with Seed Latexes S01−S04 at 70 °C

exp[a]	seed	N_{COBF}/N_{MMA} [ppm]	$\bar{n}_{COBF}$[b]	x[c]	N_p [dm_W^{-3}]	$d_p(V)$[d] [nm]	poly[e]
C011	S01	0.0	0.0	1.00	3.3×10^{18}	68	0.104
C012	S01	1.1	0.05	0.97	3.3×10^{18}	67	0.086
C013	S01	5.6	0.25	0.61	3.3×10^{18}	64	0.089
C014	S01	11.2	0.50	0.64	3.3×10^{18}	71	0.080
C015	S01	22.5	1.00	0.19	3.3×10^{18}	63	0.076
C021	S02	0.0	0.0	0.92	7.3×10^{17}	118	0.010
C022	S02	3.5	0.5	0.65	7.3×10^{17}	105	0.034
C023	S02	7.1	1.0	0.74	7.3×10^{17}	113	0.031
C024	S02	14.1	2.0	0.46	7.3×10^{17}	103	0.061
C031	S03	4.0	50	0.90	1.1×10^{16}	224	0.089
C041	S04	5.4	550	0.86	6.2×10^{14}	649	0.029

[a] The codes of the CCT polymerizations are given by C0Xx, where X refers to the seed latex used and x to the xth experiment. [b] The absolute number of COBF molecules was calculated using the phase ratio, which was a constant in all experiments, $\beta = 0.25\ dm_M^3\ dm_W^{-3}$ and a partition coefficient of $0.72\ dm_w^3\ dm_M^{-3}$. [c] Final conversion obtained from gravimetrical analysis. [d] The volume-average particle diameter. [e] Poly is the polydispersity of the particle size distribution as calculated by the Malvern software.

phase ratio $\beta = V_M/V_W$. The total volume of the organic phase includes the polymer particles and, as the partition coefficient is hardly affected by the presence of polymer in the monomer phase,[25] both monomer and polymer. The phase ratio for a seeded emulsion polymerization is given by eq 3, where V_{seed}, V_W, and $V_{MMA,aq}$ are the volume of seed latex, water, and MMA dissolved in the aqueous phase, respectively, f_p the volume fraction of polymer in the seed latex, and φ_{MMA} the actual swelling of MMA in a polymer particle.

$$\beta = \frac{V_{seed}f_p + V_{seed}f_p\varphi_{MMA} + V_{MMA,aq}}{V_{seed}(1-f_p) + V_W} \qquad (3)$$

Calculation of the phase ratio requires of the volume of seed polymer ($= V_{seed}f_p$), the volume of monomer in the polymer particles ($= V_{seed}f_p\varphi_{MMA}$), the volume of water

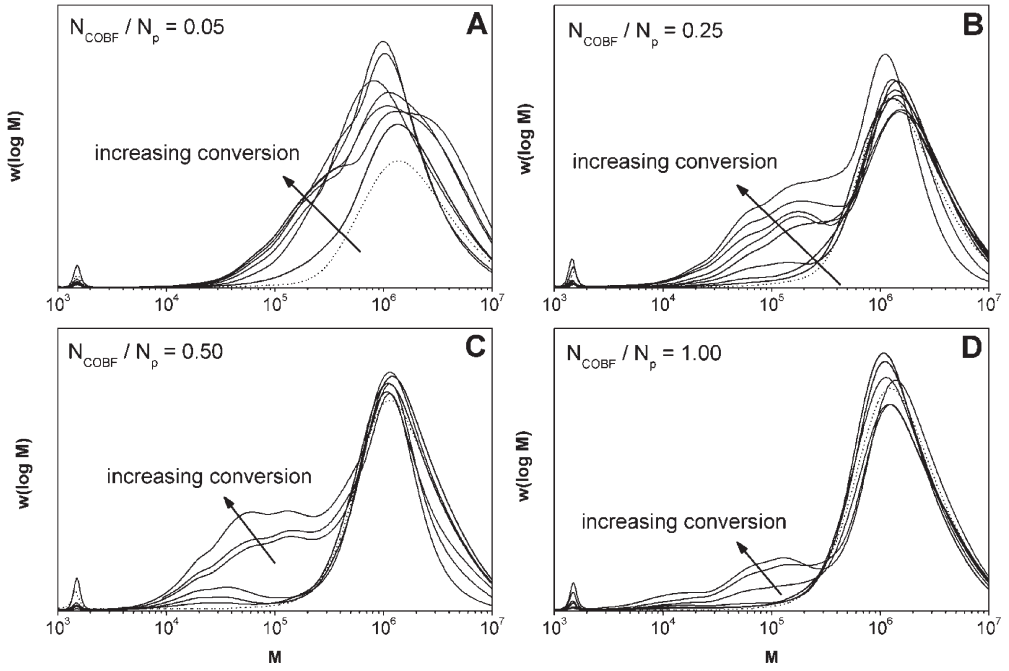

Figure 2. Evolution of the molecular weight distribution for the methyl methacrylate seeded emulsion polymerization experiments with seed latex S01 (d_p = 48 nm, Table 3) at 70 °C. Molecular weight distribution of S01 (···); molecular weight distributions of C012−C015 (Table 1) (—). All the distributions have been scaled to the amount of seed polymer.

($= V_{seed}(1 - f_p) + V_W$), and the volume of monomer in the aqueous phase, given by eq 4.

$$V_{MMA,aq} = \frac{[MMA]_{aq}^{sat} M_{MMA}[V_{seed}(1-f_p)+V_W]}{\rho_{MMA}} \left\{ \frac{\varphi_{MMA}}{\varphi_{MMA,sat}} \exp(\varphi_{MMA,sat} - \varphi_{MMA}) \right\} \quad (4)$$

In this equation, $[MMA]_{aq}^{sat}$ is the saturation solubility of MMA in the aqueous phase, M_{MMA} the molar mass of a monomer molecule, ρ_{MMA} the density of MMA, and $\varphi_{MMA,sat}$ the saturation swelling of MMA in a polymer particle. The phase ratio for all reported experiments was 0.25, corresponding to a solid content of 20%. The number of COBF molecules per particle can be calculated by using eqs 3 and 4 and a mass balance for COBF and dividing by the absolute number of polymer particles. The average numbers of COBF molecules per polymer particle ($\bar{n}_{COBF} = N_{COBF}/N_p$) for different particle diameters are presented in Figure 1.

Besides the control of the molecular weight distribution, COBF also affects the course of the emulsion polymerization. For small polymer particles, the amount of COBF required to obtain a high $\bar{n}_{COBF}$ is expected to result in low rates of polymerization as the radical entry rate is severely decreased and the exit and termination rate increased.[25−27] For large polymer particles, the amount of COBF required to obtain a low $\bar{n}_{COBF}$ would result in very high degrees of polymerization, most likely hardly indistinguishable from that of the seed latex. As the number of COBF molecules per particle strongly depends on the particle size, seed latexes with different particle sizes are required to cover the full range of $0.05 \leq \bar{n}_{COBF} \leq 500$. The experimental results of the compartmentalization experiments are summarized in Table 1.

A crucial parameter is the number of polymer particles in the polymerization. The calculations of N_{COBF}/N_p are based on the initial particle number, as obtained from the analysis of the different seed latexes S01 to S04. The poly's of the particle size distributions (PSD) after swelling and polymerization are all below 0.1, which is a good indication for a monomodal latex. The final particle diameters are within experimental error of the calculated swollen particle diameters. Both observations indicate that secondary nucleation, although in principle possible in the case of methyl methacrylate, was negligible. This in turn implies that the predetermined N_{COBF}/N_p ratio should hold throughout the course of the polymerization and that any possible effects appearing in the molecular weight distribution (MWD) are most likely ascribed to the changes in the partitioning behavior and mass transport of COBF.

The evolution of the MWDs for the experiments with $0.05 \leq \bar{n}_{COBF} \leq 1$ for the 48 nm seed particles (C012−C015) are presented in Figure 2, in which the MWDs are normalized with respect to the amount of seed polymer in the polymerization, to clearly visualize the polymer produced in the second stage. The addition of a catalytic chain transfer agent in ab initio emulsion polymerization results in a monomodal MWD.[20] When added to a seeded emulsion polymerization, with polymer particles swollen with monomer below their saturation swelling, independent of the N_{COBF}/N_p ratio, multimodal MWDs are obtained as can be clearly seen from Figure 2. For $\bar{n}_{COBF}$ = 0.05, the multimodality of the MWD is not as apparent as is the case for $\bar{n}_{COBF}$ = 0.25, 0.50, and 1.00, but still a distinct shoulder at the low molecular weight end of the distribution can be distinguished. The MWD also seems to broaden on its high molecular weight end. For $\bar{n}_{COBF}$ = 0.25, 0.50, and 1.00 the observations are comparable. A distinct set of peaks are appearing at the lower end of the distribution, whereas hardly any secondary polymer appears at the high molecular weight end. As is clearly seen in Figure 2, the multimodal character of the MWD is already present from the initial stages of the polymerization and becomes more pronounced at higher conversions. It is unlikely that the multimodality of the MWDs is caused by deactivation of the active complex due to impurities or the pH, as the chosen reaction conditions in this study

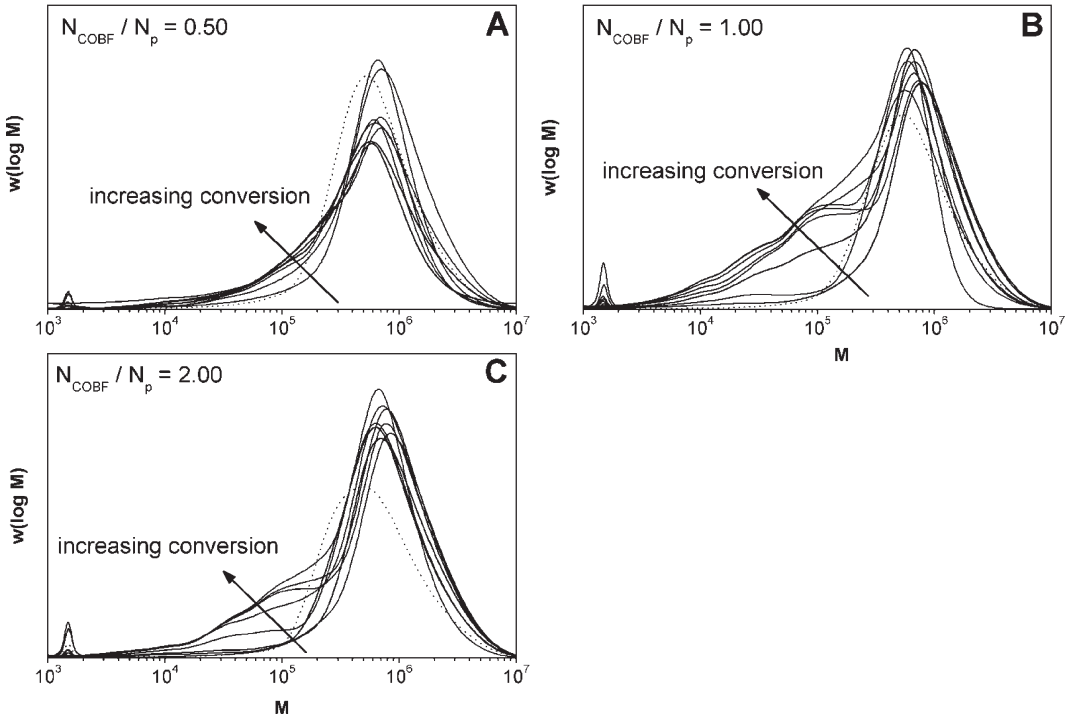

Figure 3. Evolution of the molecular weight distribution for the methyl methacrylate seeded emulsion polymerization experiments with seed latex S02 (d_p = 90 nm, Table 3) at 70 °C. Molecular weight distribution of S02 (···), molecular weight distributions of C022−C024 (Table 1) (—). All the distributions have been scaled to the amount of seed polymer.

should minimize COBF deactivation.[24] Moreover, deactivation would result in a gradual change in the MWD, yielding a virtually monomodal MWD with a very large polydispersity index, rather than a set of discrete distributions as shown here. Therefore, it was concluded that these multimodal distributions originate from the presence of different polymer populations.

It is clear that the results shown in Figure 2 do not correspond to a situation in which an *overall* COBF concentration is sufficient to describe the produced MWDs. If this were the case, then a monomodal MWD would be expected for the second-stage polymer. For $\bar{n}_{COBF}$ = 0.05. 0.25, 0.50, and 1.00 a DP_n of 404, 81, 40, and 20, respectively, was expected based on eq 2, but it is evident that this is not observed experimentally. Moreover, when the obtained MWDs from the experiments with different $\bar{n}_{COBF}$ are compared, it is evident that the location of the peaks observable in the multimodal MWD overlay. In other words, independent of the $\bar{n}_{COBF}$ and thus the total amount of COBF in the polymerization, approximately the same set of polymer populations is formed. This is counterintuitive as an increase in the amount of COBF is expected to result in a decrease of the overall average molecular weight obtained. The relative proportions of the individual contributions to the multimodal MWD are changing according to the $\bar{n}_{COBF}$ (see Figure 2). At higher $\bar{n}_{COBF}$ more lower molecular weight polymer is produced. These qualititative observations seem to point in a direction in which there are comparable reaction environments for the polymerizations with various $\bar{n}_{COBF}$, generating similar polymer populations. Comparable trends are observed for the molecular weight distributions for the experiments with $0.50 \leq \bar{n}_{COBF} \leq 2$ for the 90 nm seed particles (C022−C024) which are presented in Figure 3.

The average degrees of polymerization of the individual contributions to the multimodal MWD were estimated from the maxima in the first derivative of $w(\log M)$ with respect to log M (i.e., $d(w(\log M))/d(\log M)$), as shown in Figure 4 for the experiments C012−C015 (48 nm seed particles) and C022−C024 (90 nm seed particles). The degrees of polymerization obtained from the derivative MWD plot are presented in Table 2. For the individual MWDs that make up the multimodal MWDs, the average degrees of polymerization approximately correspond to

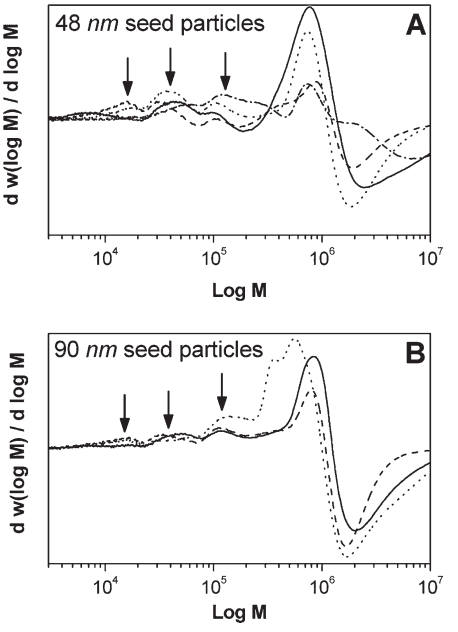

Figure 4. Plot of the differentiated molecular weight distributions ($d(w(\log M))/d(\log M)$) of the molecular weight distributions for the methyl methacrylate seeded emulsion polymerizations as reported in Figures 2 and 3. (A) The differentiated molecular weight distributions for experiments C012−C015 (Table 1) and (B) the differentiated molecular weight distributions for experiments C022−C024 (Table 1). The arrows indicate the position of the inflection points of the cumulative MWD.

Table 2. Degrees of Polymerization Obtained from Differentiated Molecular Weight Distributions for the Methyl Methacrylate Seeded Emulsion Polymerization Experiments C012−C015 (Table 1) and C022−C024 (Table 1) with Seed Latex S01 and S02 (Table 3)

	$DP_n(0)^a$	$DP_n(1)$	$DP_n(2)$	$DP_n(3)$
C012	7310	1250	497	187
C013	7460	1040	393	167
C014	8240	1030	322	163
C015	7460	1080	454	123
C022	5500	1250	393	145
C023	7310	1120	343	159
C024	8080	1170	473	160

[a] $DP_n(0)$ is predominantly the contribution of the seed polymer.

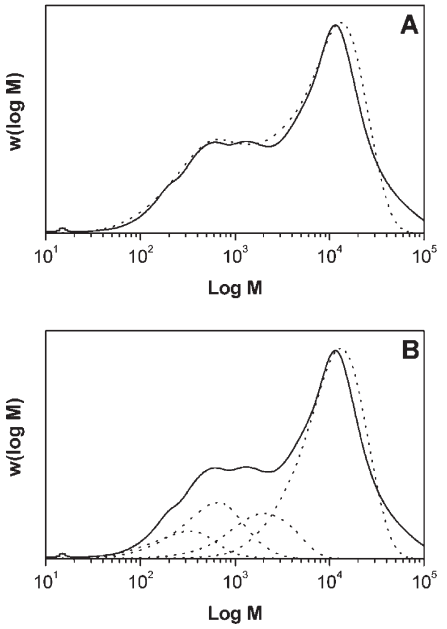

Figure 5. Final molecular weight distributions for the methyl methacrylate seeded emulsion polymerization experiment C014 (Table 1), d_p = 48 nm, $\bar{n}_{COBF}$ = 0.50 (x = 0.79). Experimental molecular weight distribution of C014 (Table 1) (—). Flory fit of the experimentally obtained molecular weight distribution (···): (A) overall distribution, (B) individual contributions. Used parameters: F_n = 1; $DP_n(0)$ = 6500, $DP_n(1)$ = 1030, $DP_n(2)$ = 322, and $DP_n(3)$ = 163; $f_0 = 1.3\times10^{-6}$, $f_1 = 1.9\times10^{-6}$, $f_2 = 7\times10^{-6}$, and $f_3 = 7\times10^{-6}$.

$DP_n \sim 1200$, 400, and 150. It is noted that the observed degrees of polymerization within the multimodal MWDs of the 48 and 90 nm particles are very similar, which suggests that there are identical reaction environments independent of the N_{COBF}/N_p ratio and apparently independent of the particle size. The latter observation is counterintuitive as for a given number of COBF molecules per particle a lower DP_n is expected in a 48 nm particle than in a 90 nm particle.

Using the obtained values for DP_n, it should be possible to fit the multimodal MWD with the individual contributions of the individual reaction environments. One possible method to fit free radical MWDs is the Flory−Schulz distribution[28] (FSD) (eq 5).[29]

$$n(i) = \frac{d[D_i]}{dt} F_n(1-S)S^{i-1} + (i-1)(1-F_n)(1-S)^2 S^{i-2} \quad (5)$$

where $[D_i]$ is the concentration of dead polymer chains with chain length i, formed by either termination or chain transfer, F_n the number fraction of chains formed by disproportionation and transfer, and S the probability of propagation (see eq 6).

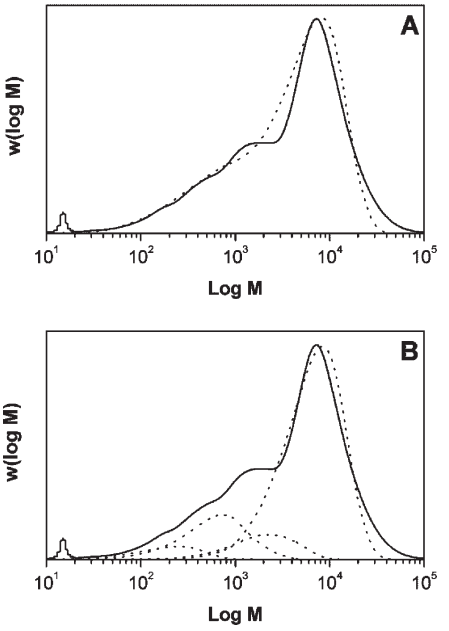

Figure 6. Final molecular weight distributions for the methyl methacrylate seeded emulsion polymerization experiment C023 (Table 1), d_p = 90 nm, $\bar{n}_{COBF}$ = 1.00 (x = 0.84). Experimental molecular weight distribution of C023 (Table 1) (—). Flory fit of the experimentally obtained molecular weight distribution (···): (A) overall distribution, (B) individual contributions. Used parameters: F_n = 1; $DP_n(0)$ = 3200, $DP_n(1)$ = 1120, $DP_n(2)$ = 343, and $DP_n(3)$ = 159; $f_0 = 0.5\times10^{-6}$, $f_1 = 0.25\times10^{-6}$, $f_2 = 1.3\times10^{-6}$, and $f_3 = 1.2\times10^{-6}$.

$$DP_n = \frac{1}{1-S} \quad \text{and} \quad F_n = \frac{k_{tr}[X] + 2k_{td}[R]}{k_{tr}[X] + 2k_{td}[R] + k_{tc}[R]} \quad (6)$$

In eq 6, k_p, k_{td}, k_{tc}, and k_{tr} are the rate coefficients of propagation, termination by disproportionation, termination by combination, and transfer, respectively, and [M] and [R] are the monomer and radical concentration, respectively. The FSD can be converted into a MWD, where f is a scaling factor which is proportionated to the amount of polymer (see eq 7).

$$w(\log i) = f_i^2 n(i) \quad (7)$$

For COBF-mediated polymerizations, bimolecular termination is negligible when compared to chain transfer and consequently F_n is ~1. The value of S is determined based on the DP_n as obtained from the differentiated MWD plots (see Table 2). The FSD fits of the final MWDs of C014 and C023 are presented in Figures 5 and 6, respectively. Three parameters can be adjusted to fit the multimodal MWD with the FSD: (i) F_n, (ii) the average degree of polymerization of the MWD, and (iii) a scaling factor to scale for the amount of polymer. As can be seen in Figures 5 and 6, a good fit of the multimodal MWD can be achieved with the contribution of four individual distributions as determined from the derivative of the MWD plot. The used average degrees of polymerization are reported in Table 2.

The evolution of the MWDs for the experiments with $N_{COBF}/N_P = 50$ and $N_{COBF}/N_P = 550$ for the 200 and 600 nm particles, respectively (C031 and C041), are presented in Figure 7. The 200 nm seed latex has been prepared in a two-step process, where in semibatch emulsion polymerization a seed latex was grown to the desired particle size of 200 nm.

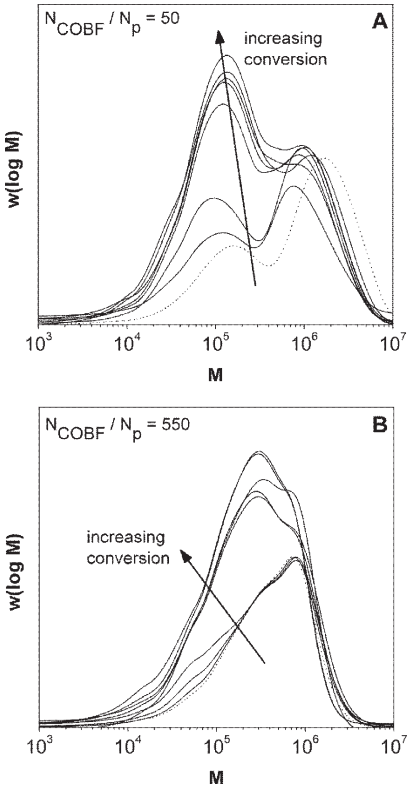

Figure 7. Evolution of the molecular weight distribution for the methyl methacrylate seeded emulsion polymerization experiments with seed latex S03 and S04 (Table 3) at 70 °C. Molecular weight distributions of C031 and C041 (Table 1) (—). All the distributions have been scaled to the amount of seed polymer.

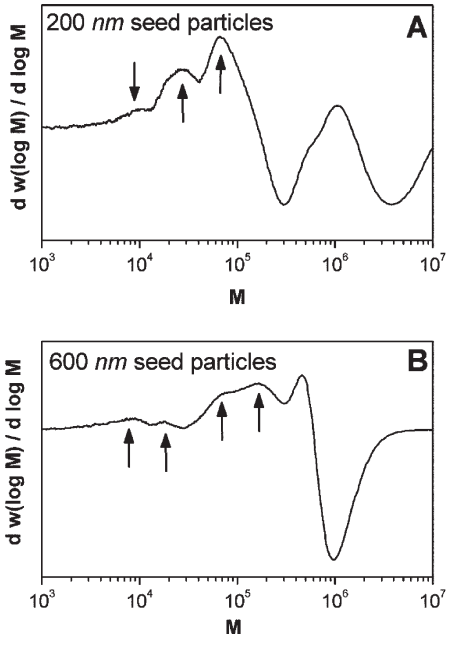

Figure 8. Plot of the differentiated molecular weight distributions (d(w(log M))/d(log M)) of the molecular weight distributions for the methyl methacrylate seeded emulsion polymerizations as reported in Figure 7. (A) The differentiated molecular weight distributions for experiments C031 (Table 1) and (B) the differentiated molecular weight distributions for experiments C041 (Table 1.) The arrows indicate the position of the inflection points of the cumulative MWD.

This two-step process is represented in the bimodality of the MWD of S03. The 600 nm seed latex has been prepared in emulsifier-free emulsion polymerization, which resulted in a very broad MWD for this seed latex.

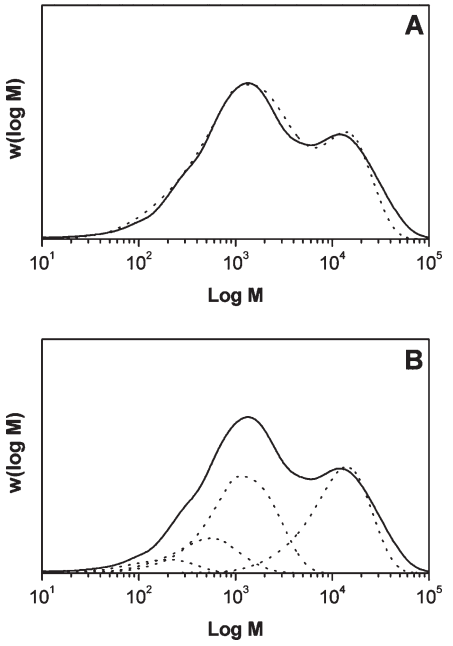

Figure 9. Final molecular weight distributions for the methyl methacrylate seeded emulsion polymerization experiment C031 (Table 1), d_p = 200 nm, $\bar{n}_{COBF}$ = 50 (x = 0.90). Experimental molecular weight distribution of C031 (Table 1) (—). Flory fit of the experimentally obtained molecular weight distribution (···): (A) overall distribution, (B) individual contributions. Used parameters: F_n = 1; $DP_n(0)$ = 5500, $DP_n(0)$ = 1500, $DP_n(1)$ = 692, $DP_n(2)$ = 275, and $DP_n(3)$ = 98; f_0 = 0.14 × 10^{-6}, f_0 = 0.36 × 10^{-6}, f_1 = 1.6 × 10^{-6}, f_2 = 1.3 × 10^{-6}, and f_3 = 1.5 × 10^{-6}.

As can be seen from Figure 7, in the evolution of the MWD of the experiment with $\bar{n}_{COBF}$ = 50 a large lower molecular weight peak is appearing. However, on closer inspection, two distinct shoulders on the low molecular weight end of this secondary peak can be observed (see Figure 8A). In the evolution of the MWD with $\bar{n}_{COBF}$ = 550 from the initial stages of the polymerization a number of distinct peaks are observed, which is illustrated in Figure 8B. Apparently even at these high numbers of COBF molecules per polymer particle, still different reaction environments are present within the polymerization system, resulting in multimodal molecular weight distributions.

Since we can determine the position of the different MWDs within the multimodal MWD by means of the differentiated plot of the MWD, we can apply the FSD to fit the experimental MWDs (see Figures 9 and 10). Comparable to the experiments with the 48 and 90 nm seed particles a good fit of the experimental MWDs can be obtained from the FSD. In the case of the 200 nm particles (C031, Figure 7A), the MWD of the seed latex was bimodal. This is represented in the FSD fit with two distributions at DP_n = 5500 and 692. The lower molecular weight part of the MWD of the seed latex is not represented in the differentiated MWD plot as it is completely covered by the MWD of the secondary formed polymer. The secondary MWDs are dominated by the distribution at DP_n = 1500. The remaining two distributions are represented as shoulders in the multimodal MWD and found at DP_n = 275 and 98. Comparable trends are observed for the 600 nm particles (C041, Figure 7B). The secondary MWDs are dominated by the distribution at DP_n = 1120, although the remaining distributions are more distinct than is the case in the 200 nm distribution (see Figure 8B).

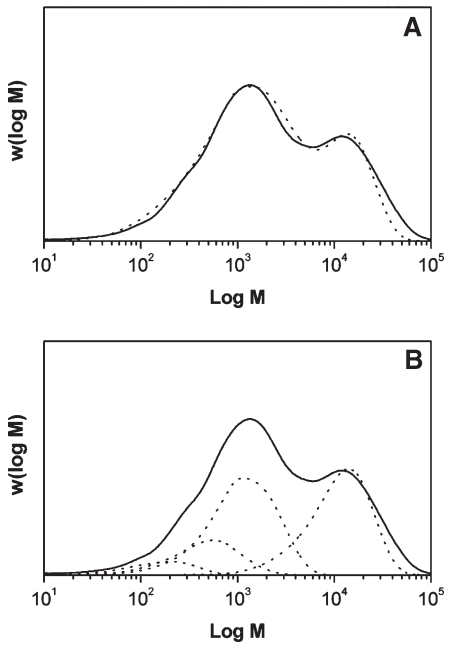

Figure 10. Final molecular weight distributions for the methyl methacrylate seeded emulsion polymerization experiment C041 (Table 1), d_p = 600 nm, $\bar{n}_{COBF}$ = 550 (x = 0.87). Experimental molecular weight distribution of C041 (Table 1) (—). Flory fit of the experimentally obtained molecular weight distribution (···): (A) overall distribution, (B) individual contributions. Used parameters: $F_n = 1$; $DP_n(0) = 3200$, $DP_n(1) = 1120$, $DP_n(2) = 343$, and $DP_n(3) = 159$; $f_0 = 0.18 \times 10^{-6}$, $f_1 = 0.7 \times 10^{-6}$, $f_2 = 1 \times 10^{-6}$, and $f_3 = 2 \times 10^{-6}$.

Evaluation of the Experimental Results. As is clear from the results presented in the previous section, the MWDs in seeded emulsion polymerization experiments cannot be described adequately by using a global COBF concentration. For proper molecular weight control a COBF molecule has to be able to enter and exit a polymer particle fast enough to prevent the formation of high molecular weight polymer. This implies that a COBF molecule has to enter a polymer particle at a time scale that has to be smaller than that of two consecutive radical entry events. In other words, in a COBF-mediated emulsion polymerization it is the entry frequency of COBF molecules that governs the MWD. If the entry frequency of a COBF molecule becomes lower than that of a radical, the MWD is governed by the entry of radicals. If the mobility of COBF is strongly reduced, as might happen for high viscosities of the polymer particles, exchange of COBF between the particles might occur very slowly or even not at all. In the latter scenario the catalytic chain transfer agent might become compartmentalized as entry and exit events are sparsely occurring. The average number of COBF molecules per particle ($= N_{COBF}/N_p$), which is governed by the polymerization recipe, can be considered as a n_{COBF} in these compartmentalized systems. At a certain moment in time a polymer particle can experience a discrete number of COBF molecules, i.e., $n_{COBF} = 0, 1, 2, 3$, etc. This also implies that at a certain instant in time there are polymer particles present with different numbers of COBF molecules. This results in the formation of a multimodal MWD where each set of polymer particles polymerizing under identical conditions (i.e., $n_{COBF} = 0, 1, 2, 3, ...$) has an individual contribution to the cumulative MWD. Note that even though the COBF molecules are compartmentalized, entry and exit events of COBF molecules might occur. This would imply that multimodal MWDs can be found in every single polymer particle as the number of COBF molecules in a single particle could be changing, however slowly, during the course of the polymerization.

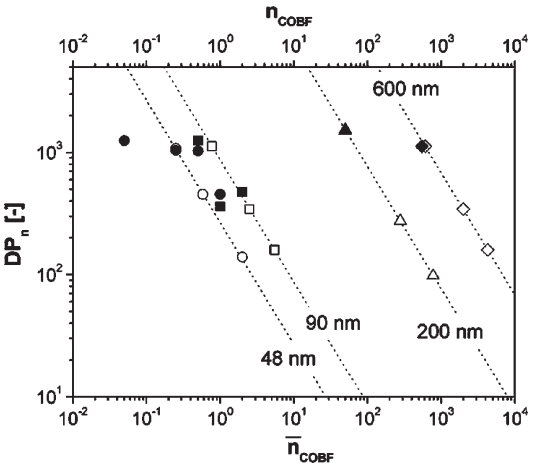

Figure 11. Average degree of polymerization as predicted by the Mayo equation as a function of the absolute number of bis[(difluoroboryl)dimethylglyoximato (COBF) molecules per seed polymer particle. Calculated DP_n for n COBF molecules in particles with a radius of 48, 90, 200, and 600 nm (···). Open symbols: $DP_{n,exp}$ (Table 2) and the corresponding number of COBF molecules (n_{COBF}) Closed symbols: $DP_{n,exp}$ of the dominant MWD (Table 2) and the average number of COBF molecules per particle ($\bar{n}_{COBF}$). Experimental observations as reported in Table 4: (○) C012−C015; (□) C022−C024; (△) C031, and (◇) C041.

Table 3. Properties of the Prepared Poly(methyl methacrylate) Seed Latexes

	PSD				MWD	
	x	d_p(V)[c] [nm]	N_p [dm_W^{-3}]	poly[d]	M_n [g mol^{-1}]	PDI
S01	0.96	48	3.3×10^{18}	0.069	7.7×10^5	2.8
S02	0.92	90	7.3×10^{17}	0.002	3.0×10^5	2.3
S03[a]	0.98	204	1.1×10^{16}	0.029	2.8×10^5	3.7
S04[b]	0.82	619	6.2×10^{14}	0.093	6.0×10^4	6.9

[a] Bimodal molecular weight distribution with a main distribution at 1.7×10^6 g mol^{-1} and a secondary distribution at 1.5×10^5 g mol^{-1}. [b] Strong tail toward the low molecular weight end of the distribution. [c] The volume-average particle diameter. [d] Poly is the polydispersity of the particle size distribution as calculated by the Malvern software.

The DP_n of a polymer particle with n COBF molecules can be calculated since a number of compartmentalized COBF molecules can be considered as a concentration within the volume of the polymer particle. This COBF concentration can subsequently be related to a DP_n using the Mayo equation. On the basis of the experimentally obtained degrees of polymerization from the FSD fits presented in Figures 5, 6, 9, and 10, a number of COBF molecules per particle can be calculated. The results of these calculations are collected in Figure 11.

Since the area underneath a MWD measured by size exclusion chromatography (SEC) corresponds to a certain mass of polymer, the modeled FSD can be used to determine an equivalent for the amount of polymer corresponding to each individual MWD. The experimentally obtained DP_n of the dominant MWD (i.e., the MWD containing most polymer) can be plotted as a function of $\bar{n}_{COBF}$ (see the closed symbols in Figure 11). The experimentally obtained DP_n of each individual MWD represented in the derivative of the multimodal MWDs can related to a concentration of COBF in a particle and consequently in a number of COBF molecules per particle (see the open symbols in Figure 11).

If we accept the notion of a statistical distribution of COBF molecules over the polymer particles, the dominant

Table 4. Experimental Conditions for the Seeded Emulsion Polymerizations of Methyl Methacrylate at 70 °C in the Presence and Absence of Bis[(difluoroboryl)dimethylglyoximato (COBF) Catalytic Chain Transfer Agent

	seed	seed [g]	MMA [mol]	water [mL]	SDS [mmol]	SBC [mmol]	COBF [10^{-4} mmol]
C011	S01	24.0	0.060	20.0	0.30	0.19	0.00
C012	S01	24.0	0.060	20.0	0.30	0.19	0.7
C013	S01	24.0	0.060	20.0	0.30	0.19	3.4
C014	S01	24.0	0.060	20.0	0.30	0.19	6.8
C015	S01	24.0	0.060	20.0	0.30	0.19	13.6
C021	S02	35.4	0.062	11.0	0.31	0.09	0.0
C022	S02	35.4	0.062	11.0	0.31	0.09	2.2
C023	S02	35.4	0.062	11.0	0.31	0.09	4.4
C024	S02	35.4	0.062	11.0	0.31	0.09	8.8
C031	S03	29.0	0.069	23.0	0.35	0.19	2.8
C041	S04	40.0	0.048	0.0	0.28	0.19	2.7

MWD should originate from the most frequently occurring n_{COBF}. Deviation from the statistical average n_{COBF} results in the formation of secondary MWDs which are lower in intensity. For $\overline{n}_{COBF} \leq 0.5$ the DP_n of the dominant MWD proves to correspond to the MWD with the highest DP_n in the multimodal MWD. If we assume that the MWD with the highest DP_n in the FSD corresponds to $n_{COBF} = 0$, then independent of the $\overline{n}_{COBF}$ the majority of the polymer particles will not experience a COBF molecule over the whole course of the polymerization. The other MWDs in the FSD consequently correspond to $n_{COBF} = 1, 2, ...$, which are less likely to occur at such low $\overline{n}_{COBF}$. For $\overline{n}_{COBF} \geq 1.0$ the dominant MWD could correspond to $n_{COBF} = 1$, where the remaining MWDs correspond to $n_{COBF} = 0, 2, 3, ...$, which are lower in intensity.

For higher $\overline{n}_{COBF}$ the conditions inside the polymer particles should approach pseudobulk conditions, which should result in a monomodal MWDs as the entry and exit of a single COBF molecule is expected to hardly affect the total COBF concentration inside a polymer particle and will consequently hardly affect the DP_n. However, the observed multimodal MWDs suggest that there are different reaction environments even at such high $\overline{n}_{COBF}$. At $\overline{n}_{COBF} = 50$ and 550 the DP_n of the dominant MWD corresponds to the calculated DP_n based on a $n_{COBF} = 50$ and 550 and the DP_n of the remaining MWDs would then originate from particles containing significantly higher n_{COBF}.

The multimodal MWDs could not be explained by either the Mayo or a modified Mayo equation for emulsion polymerization, which assume a global concentration of COBF molecules over all the polymer particles ($\overline{n}_{COBF}$), i.e., negligible resistance to mass transport of COBF. It was postulated that these multimodal MWDs might originate from a statistical distribution of COBF molecules over the particles (n_{COBF}). Polymer particles growing in the presence of 0, 1, 2, ..., n COBF molecules will exhibit MWDs of different average molecular weights, depending on the absolute number of COBF molecules inside the particle. At high instantaneous conversion inside the polymer particles, resistance against COBF exchange could be sufficiently high to result in compartmentalization of the catalytic chain transfer agent.

These observations point in the direction of two limits for catalytic chain transfer in emulsion polymerization. First, at relatively low viscosity of the particles, the particle phase can be regarded as a continuous phase with respect to catalytic chain transfer. Monomodal MWDs are produced with a DP_n which can be predicted by the modified Mayo equation (eq 8).

$$DP_n^{-1} \propto [COBF]_p \propto \overline{n}_{COBF} \quad (8)$$

Second, at relatively high viscosity of the particles, where a statistical distribution of COBF molecules over the polymer particles is present. The catalytic chain transfer agent becomes compartmentalized (eq 9).

$$DP_n^{-1} \propto [COBF]_p \propto n_{COBF} = 0, 1, 2, 3, ... \quad (9)$$

To the best of the authors knowledge, these results are the first to suggest evidence of compartmentalization in catalytic chain transfer mediated emulsion polymerization.

Conclusion

The results of this work show that in catalytic chain transfer mediated emulsion polymerization a discrete distribution of COBF molecules over the polymer particles can exist, which in turn is evidence for compartmentalization behavior of the catalytic chain transfer agent. Catalytic chain transfer seeded emulsion polymerization, with the seed particles swollen to 85% of their maximum saturation swelling, resulted in the formation of multimodal MWDs. The number-average degree of polymerization of the individual MWD of the second-stage polymer, as determined from the differentiated MWDs, proved to be qualitatively identical for different $\overline{n}_{COBF}$ for a certain seed particle size. The amount of polymer contributing to each individual MWD proved to vary with $\overline{n}_{COBF}$. For large seed particles (i.e., 200 and 600 nm) comparable observations were made. These experimental observations suggest that there are comparable reaction environments within the polymerization systems, independent of $\overline{n}_{COBF}$, that result in the formation of the multimodal MWDs. The obtained multimodal MWDs could be modeled successfully using a Flory−Schulz approach. In catalytic chain transfer mediated emulsion polymerization two limits seem to exist: one at relatively low particle viscosity where the MWD is governed by a global COBF concentration ($\overline{n}_{COBF}$) and one at relatively high particle viscosity where the MWD is governed by a discrete COBF distribution over the polymer particles (n_{COBF}).

Experimental Section

Materials. The bis(methanol) complex of COBF was prepared as described previously.[27,30] For all experiments, a single batch of catalyst was used. The intrinsic activity of the catalyst was determined by measuring the chain transfer constant in bulk polymerization of methyl methacrylate at 60 °C: $C_T = 30 \times 10^3$. Methyl methacrylate (Aldrich, 99%) was purified by passing it over a column of activated basic alumina (Aldrich). Sodium bicarbonate (SBC) (Fluka, >99%), sodium dodecyl sulfate (SDS) (Fluka, 99%), potassium persulfate (KPS) (Aldrich, >98%), and 2,2′-azobis[*N*-(2-carboxylethyl)-2-methylpropionamide] hydrate (VA-057, Wako) were used as received. Distilled deionized water was used throughout this work. Seed latexes were prepared in a 1.2 dm^3 Mettler Toledo RC1e reaction calorimeter equipped with an anchor impellor, calibration heater, T_r sensor, and sample loop. The reactor was operated in isothermal mode.

Seed Latex Preparation. Seed latex S01 was prepared by dissolving 11.0 g of SDS (3.8×10^{-2} mol) and 0.74 g of SBC (7.0×10^{-3} mol) in 710 mL (7.1 mol) of distilled deionized water. The aqueous solution was charged into the reactor, and 240 g (2.4 mol) of MMA was added subsequently. The resulting emulsion was purged with nitrogen for 1 h, while the reactor was heated to the desired reaction temperature of 70 °C. The initiator solution, prepared by dissolving 0.58 g (2.2×10^{-3} mol) of KPS in 10 mL (0.10 mol) of distilled deionized water, was injected into the reactor, and the polymerization was allowed to proceed for 1 h. After 1 h of polymerization the reactor temperature was raised to 90 °C to enhance the initiator decomposition. The final emulsion was left stirring for another 5 h, after which less than 0.5% of the initiator should remain. Finally, the seed latex was dialyzed against distilled deionized water for 2 weeks, changing the water twice a day.

Seed latex S02 was prepared by dissolving 0.61 g of SDS (2.1×10^{-3} mol) and 0.52 g of SBC (4.9×10^{-3} mol) in 510 mL (5.1 mol) of distilled deionized water. The aqueous solution was charged into the reactor, and 84.5 g (0.84 mol) of MMA was added subsequently. The resulting emulsion was purged with nitrogen for 1 h, while the reactor was heated to the desired reaction temperature of 70 °C. The initiator solution, prepared by dissolving 0.44 g (2.2×10^{-3} mol) of KPS in 10 mL (0.10 mol) of distilled deionized water, was injected into the reactor, and the polymerization was allowed to proceed for 1 h. After 1 h of polymerization the reactor temperature was raised to 90 °C to enhance the initiator decomposition. The final emulsion was left stirring for another 5 h, after which less than 0.5% of the initiator should remain. Finally, the seed latex was dialyzed against distilled deionized water for 2 weeks, changing the water twice a day.

Seed latex S03 was prepared by dissolving 0.64 g of SDS (2.2×10^{-3} mol) and 0.53 g of SBC (5.0×10^{-3} mol) in 530 mL (5.3 mol) of distilled deionized water. The aqueous solution was charged into the reactor, and 187 g (1.87 mol) of MMA was added subsequently. The resulting emulsion was purged with nitrogen for 1 h, while the reactor was heated to the desired reaction temperature of 70 °C. The initiator solution, prepared by dissolving 0.38 g (1.4×10^{-3} mol) of KPS in 10 mL (0.10 mol) of distilled deionized water, was added pseudo-instantaneously to the reactor, and the polymerization was allowed to proceed for 1 h. After 1 h of polymerization the reactor temperature was raised to 90 °C to enhance the initiator decomposition. The final emulsion was left stirring for another 5 h, after which less than 0.5% of the initiator should remain. Subsequently, 100 g of the prepared seed latex (complete conversion and a volume average particle diameter of 130 nm) was further grown in a consecutive step to the desired particle size of 200 nm. SDS (1.24 g, 4.3×10^{-3} mol) and MMA (42.6 g, 0.42 mol) were dissolved in 500 mL (0.50 mol) of distilled deionized water charged into the reactor. After swelling overnight at a temperature of 15 °C, heating to the desired reaction temperature of 70 °C and purging for 1 h, KPS (0.25 g, 9.2×10^{-4} mol), dissolved in 10 mL (0.1 mol) of distilled deionized water, was injected into the reactor. A monomer side feed of 0.278 g min^{-1} (2.8×10^{-3} mol min^{-1}) MMA was used to reach a final particle size of 200 nm. After 3 h of polymerization the reactor temperature was raised to 90 °C to enhance the initiator decomposition. Finally, the seed latex was dialyzed against distilled deionized water for 2 weeks, changing the water twice a day.

Seed latex S04 was prepared by dissolving charging 590 mL (5.0 mol) of distilled deionized water and 65 g (0.65 mol) of MMA into the reactor. The resulting emulsion was purged with nitrogen for 1 h, while the reactor was heated to the desired reaction temperature of 70 °C. The initiator solution, prepared by dissolving 0.32 g (1.2×10^{-3} mol) of KPS in 10 mL (0.10 mol) of distilled deionized water, was injected into the reactor, and the polymerization was allowed to proceed for 1 h. After 1 h of polymerization the reactor temperature was raised to 90 °C to enhance the initiator decomposition. The final emulsion was left stirring for another 5 h, after which less than 0.5% of the initiator should remain. Finally, the seed latex was dialyzed against distilled deionized water for 2 weeks, changing the water twice a day. The properties of the dialyzed latex are reported in Table 3.

Seeded Emulsion Polymerization. The seeded emulsion polymerizations were all carried out in batch, at 70 °C under a nitrogen atmosphere. In a typical recipe (Table 4, experiment C012), 0.086 g (3.0×10^{-4} mol) of SDS and 0.020 g (1.9×10^{-4} mol) of SBC were dissolved in 20 mL (0.20 mol) of distilled deionized water and charged into a three-necked round-bottom flask. 24 g of seed latex S01 and 6.0 g (6.0×10^{-2} mol) of MMA were added subsequently, and the latex was left stirring overnight to allow sufficient swelling of the polymer particles with monomer. After swelling, the latex was purged with nitrogen for 1 h and heated to the reaction temperature of 70 °C. A stock solution of 4 mg (9.5×10^{-3} mmol) of COBF in 14.6 g (0.146 mol) of MMA was prepared prior to the experiments according to the following procedure: An accurate amount of COBF was placed inside a Schlenk tube and deoxygenated by a repeated vacuum−nitrogen cycle. MMA was deoxygenated by purging with nitrogen prior to use and subsequently added to the COBF catalyst. The required amount of the stock solution (0.11 mL) was added to the swollen seed latex. The same stock solution was used throughout a series of experiments (i.e., C012−C015). The initiator, VA-057 (0.030 g, 9.3×10^{-2} mmol), was dissolved in a minimal amount of distilled deionized water (typically 1 mL), purged with nitrogen, and injected into the round-bottom flask. Samples were withdrawn periodically for further analysis. The recipes for the seeded emulsion polymerizations are collected in Table 4.

Molecular Weight Analysis. Size exclusion chromatography (SEC) was performed using a Waters 2690 separation module and a model 410 differential refractometer. A set of five Waters Styragel HR columns (HR5.0, HR4.0, HR3.0, HR1.0, HR0.5) were used in series at 40 °C. Tetrahydrofuran (THF) (Aldrich, 99%) was used as the eluent at a flow rate of 1 mL min^{-1}, and the system was calibrated using narrow molecular weight polystyrene standards ranging from 374 to 1.1×10^6 g mol^{-1}. Mark−Houwink parameters used for the polystyrene standards: $K = 1.14 \times 10^{-4}$ dL g^{-1}, $a = 0.716$ and for poly(methyl methacrylate): $K = 9.44 \times 10^{-5}$ dL g^{-1}, $a = 0.719$.

Particle Size Analysis. Particle size distributions were measured on a Malvern Zetasizer Nano. All latexes were diluted with distilled deionized water prior to the measurement. For each measurement the obtained particle size distribution data was averaged over three individual runs.

Acknowledgment. We gratefully acknowledge the financial support of the Foundation Emulsion Polymerization (SEP), useful disccusions with Dr. Greg Russell, and the comments of an anonymous referee on the discrete COBF distributions of our original manuscript.

References and Notes

(1) Zetterlund, P. B.; Okubo, M. *Macromolecules* **2006**, *39*, 8959–8967.
(2) Kagawa, Y.; Zetterlund, P. B.; Minami, H.; Okubo, M. *Macromol. Theory Simul.* **2006**, *15*, 608–613.
(3) Chern, C.-S. In *Principles and Applications of Emulsion Polymerization*, 1st ed.; Chern, C.-S., Ed.; Wiley-Interscience: Hoboken, NJ, 2008.
(4) Gilbert, R. G. In *Emulsion Polymerization: A Mechanistic Approach*; Gilbert, R. G., Ed.; Academic Press Limited: London, 1995.
(5) Cunningham, M. F. *Prog. Polym. Sci.* **2008**, *33*, 365–398.
(6) Moad, G.; Rizzardo, E.; Thang, S. H. *Acc. Chem. Res.* **2008**, *41*, 1133–1142.
(7) Zetterlund, P. B.; Kagawa, Y.; Okubo, M. *Chem. Rev.* **2008**, *108*, 3747–3794.

(8) Braunecker, W. A.; Matyjaszewski, K. *Prog. Polym. Sci.* **2007**, *32*, 93–146.
(9) Maehata, H.; Liu, X.; Cunningham, M. F. *Macromol. Rapid Commun.* **2008**, *29*, 479–484.
(10) Zetterlund, P. B.; Nakamura, T.; Okubo, M. *Macromolecules* **2007**, *40*, 8663–8672.
(11) Zetterlund, P. B.; Okubo, M. *Macromol. Theory Simul.* **2008**, *16*, 221–226.
(12) Delaittre, G.; Charleux, B. *Macromolecules* **2008**, *41*, 2361–2367.
(13) Simms, R. W.; Cunningham, M. F. *Macromolecules* **2008**, *41*, 5148–5155.
(14) Enikolopyan, N. S.; Smirnov, B. R.; Ponomarev, G. V.; Belgovskii, I. M. *J. Polym. Sci., Part A: Polym. Chem.* **1981**, *19*, 879–889.
(15) Gridnev, A. *J. Polym. Sci., Part A: Polym. Chem.* **2000**, *38*, 1753–1766.
(16) Gridnev, A. A.; Ittel, S. D. *Chem. Rev.* **2001**, *101*, 3611–3659.
(17) Heuts, J. P. A.; Roberts, G. E.; Biasutti, J. D. *Aust. J. Chem.* **2002**, *55*, 381–398.
(18) Karmilova, L. V.; Ponomarev, G. V.; Smirnov, B. R.; Belgovskii, I. M. *Russ. Chem. Rev.* **1984**, *53*, 223–235.
(19) Davis, T. P.; Haddleton, D. M.; Richards, S.N. J. *Macromol. Sci., Rev. Macromol. Chem.* **1994**, *C34*, 234–324.
(20) Davis, T. P.; Kukulj, D.; Haddleton, D. M.; Maloney, D. R. *Trends Polym. Sci.* **1995**, *3*, 365–373.
(21) Mayo, F. R. *J. Am. Chem. Soc.* **1943**, *65*, 2324–2329.
(22) Smeets, N. M. B.; Heuts, J. P. A.; Meuldijk, J.; van Herk, A. M. *J. Polym. Sci., Part A: Polym. Chem.* **2008**, *46*, 5839–5849.
(23) Vanzo, E.; Marchessault, R. H.; Stannett, V. *J. Colloid Sci.* **1965**, *20*, 62–71.
(24) Smeets, N. M. B.; Meda, U. S.; Heuts, J. P. A.; Keurentjes, J. T. F.; van Herk, A. M.; Meuldijk, J. *Macromol. Symp.* **2007**, *259*, 406–415.
(25) Kukulj, D.; Davis, T. P.; Suddaby, K. G.; Haddleton, D. M.; Gilbert, R. G. *J. Polym. Sci., Part A: Polym. Chem.* **1997**, *35*, 859–878.
(26) Smeets, N. M. B.; Heuts, J. P. A.; Meuldijk, J.; Cunningham, M. F.; van Herk, A. M. *J. Polym. Sci., Part A: Polym. Chem.* **2009**, *19*, 5078–5089.
(27) Suddaby, K. G.; Haddleton, D. M.; Hastings, J. J.; Richards, S. N.; O'Donnell, J. P. *Macromolecules* **1996**, *29*, 8083–8091.
(28) Flory, P. J. In *Principles of Polymer Chemistry*, 1st ed.; Flory, P. J., Ed.; Cornell University Press: Ithaca, NY, 1953.
(29) Russell, G. T. *Aust. J. Chem.* **2002**, *55*, 399–414.
(30) Bakač, A.; Brynildson, M. E.; Espenson, J. H. *Inorg. Chem.* **1986**, *25*, 4108–4114.